Key Engineering Materials Vols. 274-276 (2004) pp. 295-300
online at http://www.scientific.net

Mechanical Anisotropy of Superplastic Ti_3Al Based Alloy

K. L. Yang[1,2,a], J. C. Huang[1,b] and S. C. Chen[3,b]

[1] Inst. of Materials Sci. and Eng., National Sun Yat-Sen University, Kaohsiung, Taiwan 804

[2] Dept. of Electronic Eng., Kao-Yuan Institute of Technology, Luju, Kaohsiung County, Taiwan 821

[3] Dept. of Aeronautics and Mechanical Eng., Chinese Air Force Academy, Gangshan, Kaohsiung County, Taiwan 820

[a] m8736604@student.nsysu.edu.tw, [b] jacobc@mail.nsysu.edu.tw

Keywords: Mechanical anisotropy, Ti_3Al alloy, Low temperature superplasticity, Schimid factor

Abstract. The mechanical anisotropy in super α_2 Ti_3Al based alloys during low temperature superplasticity are explored. The alloy contains DO_{19} hexagonal α_2 grains ~2.2 μm in grain size uniformly distributed in the ordered BCC β matrix. Although the alloy exhibits superior superplastic elongations over 1000% at 920-1000°C, the elongation drops appreciably to 600% at 900°C, 380% at 850°C and 150% at 750°C. Mechanical anisotropy is observed, and lower flow stresses and higher tensile elongations are obtained in the 45° specimen as loaded at 25 to 960°C. The texture characteristics appear to impose significant influence on the mechanical anisotropy at temperatures below 900°C (under the dislocation creep condition). At loading temperatures higher than 900°C (under the superplastic flow condition), the anisotropy effect was less pronounced and the grain orientation distribution become basically random in nature. Rationalizations for the mechanical anisotropy in terms of Schimid factor calculations for the major and minor texture components in the α_2 and β phases provide consistent explanations for the deformation behavior at lower temperatures as well as the initial straining stage at higher temperatures.

Introduction

Ti_3Al based intermetallic alloys have the advantages of both superior high temperature properties and low density, which are highly attractive for aerospace and aircraft applications [1]. However, Ti_3Al based alloys are known to be brittle and have low toughness at low temperatures because of the DO_{19} ordered hexagonal crystal structure. By adding the β-stabilizing elements such as Nb, V, Mo, etc., or receiving thermomechanical treatments to reduce the grain sizes, the Ti_3Al based alloys with a duplex DO_{19} ordered hexagonal α_2 and ordered or disordered BCC β phase at temperatures below the β-transus temperature would exhibit much acceptable formability.

The main slip systems are the <a> type dislocations in the prism, pyramidal and basal planes, plus the <c+a> type dislocations in the pyramidal plane. For the DO_{19} hexagonal α_2 phase with the c/a ratio less than the ideal value, the <a> type dislocations in the prism planes are the major system, and in basal plane and the pyramidal plane are the secondary slip systems. Meanwhile, the <c+a> type dislocations could improve the ductility at temperatures above 800°C [2]. As for the β phase, dislocations on the {110}<111> systems are active, making β a more deformable phase, which has been regarded as the strain accommodation carrier [3].

To date, there have been a number of reports on the superplastic behavior of Ti_3Al based alloys [4-7], confirming that the Ti_3Al based alloys exhibited admirable high temperature superplasticity (HTSP) of elongation greater than 1200% [5,7]. In general, most Ti_3Al based alloys [5-7] exhibited superplastic behavior at higher temperatures between 920-1000°C (~0.64 T_m, where T_m for Ti_3Al is 1953 K) and lower strain rates between 10^{-4}-10^{-5} s^{-1}. Superplastic forming at these temperatures requires expensive tooling and leads to oxidation during long superplastic forming time. Therefore, reduction in the temperature range to <0.6 T_m would be attractive. There have been very limited studies reporting the low temperature superplasticity (LTSP) in Ti_3Al alloys.

Although LTSP in TiAl and Ti_3Al based alloys with submicrocrystalline structure could occur at temperatures below 900°C [8], their deformation mechanism, anisotropy behavior and texture evolution are still inadequately understood. In this research, the LTSP behavior in super α_2 Ti_3Al-Nb alloys at 800 ± 100°C (0.55 ± 0.05 T_m) is examined. The mechanical anisotropy at higher (950 ± 50°C) and lower (800 ± 100°C) temperatures are explored and compared.

Experimental Methods

The super α_2 material was supplied by Rockwell Internatioal, USA, originally fabricated by Timet, USA, with a nominal composition of Ti-25%Al-10%Nb-2%V-1%Mo (in at%). The as-received Ti_3Al thin sheet specimen was 2 mm in thickness.

Systematic LTSP tensile tests were performed under the constant-crosshead-speed tests at 700-850°C with initial strain rates of $8x10^{-5}$, $2x10^{-4}$, $5x10^{-4}$ s^{-1}, and $1x10^{-2}$ s^{-1},respectively. For studying the anisotropic superplasticity, the tensile specimens were machined with the loading axis aligned along a direction parallel (0°), perpendicular (90°), or 45° to the rolling directions, respectively. Anisotropic tensile tests were performed at 25, 750, 850 and 920°C. To retain the microstructure of superplastically loaded specimens, the specimens should be rapidly cooled. However, to take account of safety and to prevent oxidation in air, high temperature furnace could not be opened at temperatures above 500°C for allowing cooling by liquid nitrogen. To achieve rapid cooling, it is necessary to use a thin steel pipe to insert into the furnace so that liquid nitrogen could be purged via the pipe at a pressure of 2 kg/cm^2.

The as-received and superplastically loaded specimens were milled using emery papers with water, then polished using 0.1-0.3 μm Al_2O_3 suspensions. After that, specimens were etched with the Kroll's reagent (10% HF + 5% HNO_3 + 85% H_2O) to attain the microstructural information by scanning electron microscopy (SEM). From the SEM micrographs, the grain structure and grain sizes can be roughly revealed. Microtextures of both the as-received and post-SP specimens were determined by electron backscattered diffraction (EBSD). Pole figures are used to investigate the texture change during superplastic deformation. The EBSD system applied is the Oxford Instrument LinkOpal^{TM} interfaced to a field emission gun JSM-6330TF SEM.

Results and Discussions

Microstructure characterization. The SEM microstructure of the as-received material is shown in Fig. 1. The alloy consists of mixture of α_2 (the darker phase) and β (the lighter phase) phases. The coarse α_2 plates (measuring ~10x4x2 μm) and fine spherical α_2 particles (measuring ~2 μm) are nearly random dispersed within the β matrix. Assuming that the α_2 grains are spherical particles, the average effective grain size of the α_2 grains is 2.2 μm.

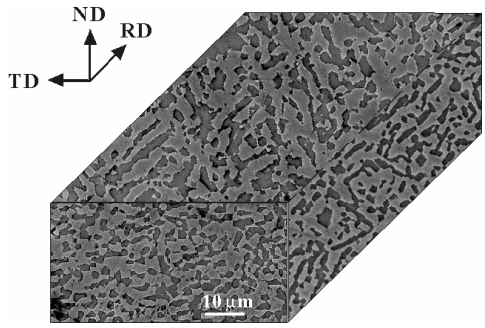

Fig. 1 SEM micrograph showing the three-dimensional microstructure of the as-received material.

Mechanical tests. The yield strength (YS) and the ultimate tensile strength (UTS) for the 0° specimen was extracted to be 950 ± 30 MPa and 1100 ± 40 MPa, respectively. The data lie between the higher values for the 90° specimen and the lower values for the 45° one, as compiled in Table 1. The 45° specimens always show lower tensile strengths and higher elongations.

Table 1 Anisotropic tensile test results performed at room temperature and $3x10^{-3}$ s^{-1}

Orientation to RD	Yield stress (MPa)	Ultimate tensile strength (MPa)	Elongation (%)
0^o	950 ± 30	1100 ± 40	5
45^o	900 ± 40	1020 ± 50	6
90^o	1150 ± 30	1220 ± 50	2

Table 2 Summary of tensile properties at different strain rates and temperatures

Temperatures (^{o}C)	$8x10^{-5}$ s^{-1}	$2x10^{-4}$ s^{-1}	$5x10^{-4}$ s^{-1}	$1x10^{-2}$ s^{-1}	m-value
700	28%	20%	26%	16%	0.2
750	141%	131%	39%	28%	0.2
800	100%	130%	123%	84%	0.33
850	186%	200%	333%	145%	0.33
900	643%	595%	451%	-	0.50
960	980%	1500%	683%	-	0.68
1000	684%	875%	610%	-	0.63

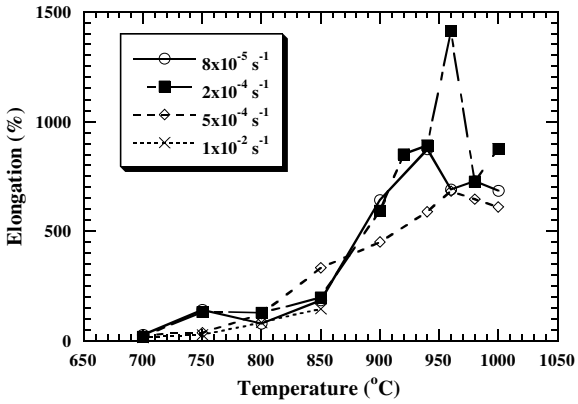

Fig. 2 The dependence of superplastic elongations as a function of loading temperature at various initial strain rates.

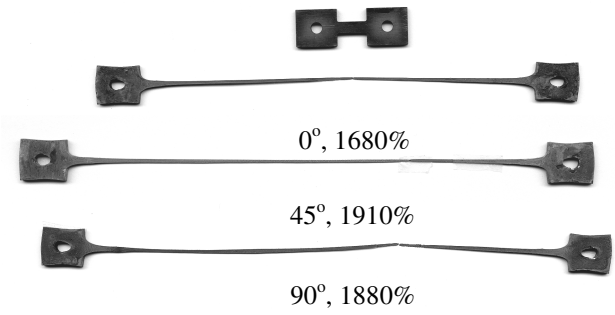

Fig. 3 Representative anisotropic tensile specimens loaded at 920^{o}C and $5x10^{-4}$ s^{-1}.

The superplastic tensile tests were performed at temperatures over 700-850^{o}C with initial strain rates from $8x10^{-5}$ to $5x10^{-4}$ s^{-1}. Table 2 summarizes the results of tensile elongations and strain rate sensitivities at elevated temperatures together with some of the previous results for HTSP [7]. The dependence of superplastic elongations as a function of test temperature at an initial strain rate of $8x10^{-5}$ to $1x10^{-2}$ s^{-1} is shown in Fig. 2. The highest LTSP elongation of 333% was obtained at 850^{o}C and an initial strain rate of $5x10^{-4}$ s^{-1}. However, the elongation decreases abruptly as loading temperatures fell below 750^{o}C.

Table 3 Anisotropic tensile test results performed at elevated temperatures and of $5x10^{-4}$ s^{-1}

Orientation to RD	750°C	850°C	920°C	960°C
0°	39%	333%	1680%	1200%
45°	155%	380%	1910%	1290%
90°	38%	310%	1880%	1130%

The anisotropy tensile results conducted at 750 to 960°C are listed in Table 3. Higher elongations for the 45° specimens are obtained at all temperatures studied. The anisotropy behavior in terms of tensile elongation appears to be most pronounced at 750°C, and gradually diminishing with increasing loading temperature up to 960°C. Figure 3 represents the fracture morphology of the specimens loaded at 920°C. Note that the 1910% occurred in the 45° specimen is even higher than the previously reported highest superplastic elongation of 1500% for the Ti_3Al based alloy [7]. And the current temperature and strain rate of 920°C and $5x10^{-4}$ s^{-1} are also lower and faster than the previous one of 960°C and $2x10^{-4}$ s^{-1}.

Textures present in the as-received and SP loaded specimens. In the current study, the strong {100}<011> rotated cube texture should be a result of recrystallization, while the $\{111\}<2\bar{1}\bar{1}>$ and {110}<001> textures ought to be the retained ones originated from thermomechanical treatment involving complicated direct- and cross-rolling practices. From literatures [9-11], it was suggested that the rolling texture in the α_2 phase is mainly the basal {0001} fiber texture. Similarly, in our current study, the basal texture is also retained from the rolling texture and deviated the perfect (0001)<uvtw> within 10°. The strong $\{11\bar{2}0\}<\bar{1}100>$, the $\{0001\}<11\bar{2}0>$ and $\{0001\}<\bar{1}100>$ basal textures as well as $\{11\bar{2}0\}$<0001>, and other multiple non-basal textures coexisting in our starting material should result from recrystallization.

After superplastic loading at 750°C, some of the β grains concentrate rapidly into the $\{111\}<2\bar{1}\bar{1}>$ orientation. With increasing loading temperature to 850°C, or even 920°C, GBS becomes increasingly dominant , the $\{111\}<2\bar{1}\bar{1}>$ intensity is decreased. At the later straining stage at 920°C, there is basically no apparent preferred orientation. As for the α_2 grains, the $\{11\bar{2}0\}$<0001> recrystallization texture present in the starting material become weakened upon loaded at 750°C. The α_2 grains have a tendency to lead the (0001) plane parallel to the rolling plane (similar to the situation during rolling), and the near $<\bar{1}100>$ orientation, or more precisely the $<\bar{4}130>$ orientation, tends to align along the tensile axis. With increasing loading temperature to 850°C, or even 920°C, $\{11\bar{2}0\}$<0001> soon becomes diminished with minor basal typed textures ({0001} plane, $\{0001\}<\bar{4}310>$, $\{0001\}<11\bar{2}0>$, and $\{0001\}<10\bar{1}0>$). At the later straining stage at 920°C, even the basal textures also evolve to extremely weak.

Influence from textures on the mechanical anisotropy. Grains with equiaxed shape are suitable for grain boundary sliding and would not give rise to pronounced superplastic anisotropy. On the other hand, elongated and hard grains acting as barriers to grain boundary sliding would give rise to superplastic anisotropy [12]. In the current starting alloy, the grain structures are mostly near equiaxed, the microstructure grain shape effect on the mechanical anisotropy is postulated to be minor.

Dislocation mobility would significantly affect the ductility at temperatures below 800°C (under the dislocation creep condition), and during the initial stage of the deformation at higher temperatures (under the superplastic flow condition). To consider about the dislocation mobility in the β and α_2 phases, the Schmid factor is an important indication [13]. It is well known that dislocations would

tend to slip along the system with a higher Schmid factor. The BCC β phase is more deformable than the hexagonal α_2 phase. The dislocation motion and dislocation accommodation process would be operative more readily in the β phase. In addition, the Schmid factor effect in the β phase may be more important than that in the α_2 phase due to the higher initial volume fraction (~60%) of the β phase.

For the BCC β phase, the Schmid factor analysis was only carried out on the dislocations acting on the main $\{110\}\langle\bar{1}11\rangle$ slip system. For the texture existed in the β phase, i.e., $\{100\}\langle 110\rangle$, $\{111\}\langle 2\bar{1}\bar{1}\rangle$, and $\{0\bar{1}1\}\langle 001\rangle$, the Schmid factors are overall highest when the stress is acted along the 45^{o} direction against the RD direction (Table 4), leading to a lower flow stress and a highest elongation. There are 12 slip systems of the kind in the β phase. If one set of the dislocation would be blocked while loading, dislocations would easily continue to cross slip into another set of slip systems.

Table 4 Schmid factors calculated for the β phase

Orientation to RD	Major texture		Minor texture
	$\{100\}\langle 110\rangle$	$\{111\}\langle 2\bar{1}\bar{1}\rangle$	$\{0\bar{1}1\}\langle 100\rangle$
	Acting on the $\{110\}\langle\bar{1}11\rangle$ slip system		
0^{o}	0.14	0.18	0.27
45^{o}	0.27	0.17	0.17
90^{o}	0.14	0.14	0.14

Table 5 Schmid factors calculated for the α_2 phase

Orientation to RD	Major texture			Minor texture								
	$\{11\bar{2}0\}\langle 0001\rangle$			$\{11\bar{2}0\}\langle\bar{1}100\rangle$			$\{0001\}\langle\bar{1}100\rangle$			$\{0001\}\langle 11\bar{2}0\rangle$		
	Acting on the main slip systems											
	$\{10\bar{1}0\}\langle 11\bar{2}0\rangle$	$\{0001\}\langle 11\bar{2}0\rangle$	$\{10\bar{1}\bar{1}\}\langle 11\bar{2}0\rangle$	$\{10\bar{1}0\}\langle 11\bar{2}0\rangle$	$\{0001\}\langle 11\bar{2}0\rangle$	$\{10\bar{1}\bar{1}\}\langle 11\bar{2}0\rangle$	$\{10\bar{1}0\}\langle 11\bar{2}0\rangle$	$\{0001\}\langle 11\bar{2}0\rangle$	$\{10\bar{1}\bar{1}\}\langle 11\bar{2}0\rangle$	$\{10\bar{1}0\}\langle 11\bar{2}0\rangle$	$\{0001\}\langle 11\bar{2}0\rangle$	$\{10\bar{1}\bar{1}\}\langle 11\bar{2}0\rangle$
0^{o}	0	0	0	0.29	0	0.20	0.29	0	0.20	0.29	0	0.20
45^{o}	0.15	0.29	0.21	0.15	0.29	0.21	0.33	0	0.23	0.33	0	0.23
90^{o}	0	0.29	0.20	0	0	0	0.29	0	0.20	0.29	0	0.20

The main slip systems in the DO_{19} α_2 phase include mainly <a> type dislocation acting on (i) prismatic $\{10\bar{1}0\}$, (ii) basal $\{0001\}$, and (iii) pyramidal $\{10\bar{1}\bar{1}\}$ planes. In the Ti_3Al alloy, the primary slip system is the <a> type dislocation acting on the prism plane, i.e. $\{10\bar{1}0\}\langle 11\bar{2}0\rangle$ since the c/a ratio is less than the ideal value [14]. From the calculated Schmid factor values listed in Table 4, the Schmid factors for the α_2 phase in average are also highest in the 45^{o} specimens, also favoring a lower flow stress and a highest elongation. It could be seen that the Schmid factors in the major textures in the 0^{o} specimen are zero. As a result, dislocation motions could only occur in grains of the minor textures or after the α_2 grains rotate into a position with (0001) parallel to the rolling plane.

The {0001} basal texture formation during tensile loading might be similar to that in the basal rolling texture. The <a> typed dislocations can slip on the {0001}, $\{10\bar{1}0\}$, and $\{10\bar{1}\bar{1}\}$ planes, leading to the formation of the basal texture [15]. After the α_2 grains rotate into the {0001}<uvtw> orientation, the Schmid factors increase. As tabulated in Table 5, the Schmid factors of <a>-typed dislocations acting on the three main slip systems in the basal $\{0001\}\langle\bar{1}100\rangle$ and $\{0001\}\langle 11\bar{2}0\rangle$ textures are greater than those in the $\{11\bar{2}0\}\langle 0001\rangle$ and $\{11\bar{2}0\}\langle\bar{1}100\rangle$ textures. Consequently,

once the basal typed textures are formed in the α_2 grains during tensile loading, dislocation glide and climb could proceed more thoroughly in the dislocation creep dominating stage at 700-850°C.

At 900-1000°C under the smooth grain boundary sliding stage, the rotation of α_2 grains are continuously operating and the orientations are distributed more and more randomly. However, texture effects should still be considered even in the superplastic flow condition [14,16]. The textured Ti alloys have been shown to exhibit slightly greater ductility as compared with the textureless alloy under the GBS-controlling regime. Nevertheless, the existing texture can only impose influence during the initial stage; the extensive GBS would eventually lead to random grain orientation at later stage. The mechanical anisotropy can at most account for ±10% in flow stress or SP elongation under the optimum superplastic region.

Summary

(1) Although the super α_2 alloy exhibited superior superplastic elongations of 1500% at 960°C, the elongation dropped appreciably to 600% at 900°C, 330% at 850°C and 140% at 750°C.
(2) After superplastic loading at 750 to 920°C, the $\{11\bar{2}0\}<0001>$ texture present in the α_2 phase of the starting material becomes extremely weaker, and the (0001) plane tends to lie parallel to the rolling plane. The orientations in the β phase are distributed more randomly than the α_2 phase and some of the β grains tend to concentrate into the $\{111\}<2\bar{1}\,\bar{1}>$ orientation.
(3) Higher elongations and lower flow stresses are consistently obtained in the 45° specimens as tensile loaded at 25 to 960°C.
(4) The Schmid factors for the 45° specimens are the highest in the α_2 and β phases. It provides the reasonable origin for the mechanical anisotropy.

Acknowledgement

The project is sponsored by the National Science Council of Taiwan, ROC, under the contrast no. NSC 91-2216-E-110-005.

References

[1] C. H. Ward: Int. Mater. Rev. Vol. 38 (1993), p. 79.
[2] H. A. Lipsitt, D. Shechtman and R. E. Schafrik: Metall. Trans. A Vol. 11A (1980), p. 1369.
[3] D. Banerjee, T. K. Nandy and A. K. Gogia: Scripta Metall. Vol. 21 (1987), p. 597.
[4] A. Dutta and D. Banerjee: Scripta Metall. Mater. Vol. 24 (1990), p. 1319.
[5] J. H. Kim, C. G. Park, T. K. Ha and Y. W. Chang: Mater. Sci. Eng. Vol. A269 (1999), p. 197.
[6] H. S. Yang, P. Jin, E. Dalder and A. K. Mukherjee: Scripta Metall. Vol. 25 (1991), p. 1223.
[7] H. C. Fu, J. C. Huang, T. D. Wang and C. C. Bampton: Acta Mater. Vol. 46 (1998), p. 465.
[8] R. M. Imayev, N. K. Gabdullin, G. A. Salishchev, O. N. Senkov, V. M. Imayev and F. H. Froes: Acta Mater. Vol. 47 (1999), p. 1809.
[9] W. P. Hon, S. K. Wu and C. H. Koo: Mater. Sci. Eng. Vol. A131 (1991), p. 85.
[10] D. B. Knorr and N. S. Stoloff: Mater. Sci. Eng. Vol. A123 (1990), p. 81.
[11] S. Suwas and R. K. Ray: Acta Mater. Vol. 47 (1999), p. 4599.
[12] D. S. McDarmaid, A. W. Bowen and P. G. Partridge: J. Mater. Sci. Vol. 19 (1984), p. 2378.
[13] Y. T. Wu and C. H. Koo: Intermetallics Vol. 5 (1997), p. 29.
[14] V. M. Imayev, G. A. Salishev, M. R. Shagiev, A. V. Kuznetsov, R. M. Imayev, O. N. Senkov and F. H. Foes: Scripta Mater. Vol. 40 (1999), p. 183.
[15] B. Bai, H. S. Yang, N. Chen and A. K. Mukherjee: Scripta. Mater. Vol. 40 (1999), p. 1079.